BMP-binding protein twisted gastrulation is required in mammary gland epithelium for normal ductal elongation and myoepithelial compartmentalization

Cynthia L. Forsman [a,b,c], Brandon C. Ng [a,b], Rachel K. Heinze [a,b], Claire Kuo [a,b], Consolato Sergi [d], Rajaram Gopalakrishnan [e], Douglas Yee [c,f], Daniel Graf [g], Kathryn L. Schwertfeger [c,h], Anna Petryk [a,b,c,*]

[a] Department of Genetics, Cell Biology and Development, University of Minnesota, Minneapolis, MN 55455, USA
[b] Department of Pediatrics, University of Minnesota, Minneapolis, MN 55455, USA
[c] Masonic Cancer Center, University of Minnesota, Minneapolis, MN 55455, USA
[d] Department of Laboratory Medicine & Pathology, University of Alberta, Alberta, Canada T6G 2B7
[e] Diagnostic/Biological Sciences, School of Dentistry, University of Minnesota, Minneapolis, MN 55455, USA
[f] Department of Medicine, University of Minnesota Medical School, Minneapolis, MN 55455, USA
[g] Institute of Oral Biology, Faculty of Medicine, University of Zurich, Zurich, Switzerland
[h] Department of Laboratory Medicine and Pathology, University of Minnesota, Minneapolis, MN 55455, USA

ARTICLE INFO

ABSTRACT

Bone morphogenetic proteins (BMPs) are involved in embryonic mammary gland (MG) development and can be dysregulated in breast cancer. However, the role BMPs play in the postnatal MG remains virtually unknown. BMPs are potent morphogens that are involved in cell fate determination, proliferation, apoptosis and adult tissue homeostasis. Twisted gastrulation (TWSG1) is a secreted BMP binding protein that modulates BMP ligand availability in the extracellular space. Here we investigate the consequences of TWSG1 deletion on development of the postnatal MG. At puberty, *Twsg1* is expressed in the myoepithelium and in a subset of body cells of the terminal end buds. In the mature duct, *Twsg1* expression is primarily restricted to the myoepithelial layer. Global deletion of *Twsg1* leads to a delay in ductal elongation, reduced secondary branching, enlarged terminal end buds, and occluded lumens. This is associated with an increase in luminal epithelial cell number and a decrease in apoptosis. In the MG, pSMAD1/5/8 level and the expression of BMP target genes are reduced, consistent with a decrease in BMP signaling. GATA-3, which is required for luminal identity, is reduced in $Twsg1^{-/-}$ MGs, which may explain why K14 positive cells, which are normally restricted to the myoepithelial layer, are found within the luminal compartment and shed into the lumen. In summary, regulation of BMP signaling by TWSG1 is required for normal ductal elongation, branching of the ductal tree, lumen formation, and myoepithelial compartmentalization in the postnatal MG.

© 2012 Elsevier Inc. All rights reserved.

Introduction

Bone morphogenetic proteins (BMPs), members of the transforming growth factor β (TGFβ) superfamily, are morphogens that play diverse roles during embryonic development and postnatal life (Wagner et al., 2010). BMPs have been implicated in regulating tissue homeostasis in physiological states as well as pathological ones, such as cancer, by mediating basic biological processes including cell proliferation, migration, differentiation, apoptosis, and epithelial–stromal interactions (Buijs et al., 2012; Singh and Morris, 2010; Virtanen et al., 2011; Wang et al., 2011a). There is growing evidence that developmental programs, which are important during embryonic development and adult homeostasis, can be inappropriately reactivated during the initiation and progression of cancer (Bowman and Nusse, 2011; McEvoy et al., 2011; Wang et al., 2011b). Specifically, BMPs play important roles during embryonic mammary gland (MG) development and have been shown to be dysregulated in breast and other cancers often acting as a tumor suppressor or tumor promoter depending on dosage, time and tissue of expression (Bailey et al., 2007; Beppu et al., 2008; Cho et al., 2006; Hens et al., 2007; Liu et al., 2008). Given that developmental programs, such as BMP mediated processes, are co-opted or exploited by tumorigenic cells, it is important to understand what roles BMPs play during normal MG development and how their activity is regulated.

* Correspondence to: Department of Pediatrics, University of Minnesota, East Building Room MB671, 2450 Riverside Avenue, Minneapolis, MN 55454, USA. Fax: +1 612 626 5262.
E-mail address: petry005@umn.edu (A. Petryk).

In both humans and mice, the MG is a dynamic organ that responds and develops over the lifetime of the female. Embryonic development establishes the rudimentary ductal tree that during puberty, pregnancy and lactation undergoes complex morphological changes (Hens and Wysolmerski, 2005; Hovey and Trott, 2004). In the mouse, MG development begins around embryonic day 10.5 (E10.5) when epithelial thickenings form placodes, which further thicken and invaginate as they respond to inductive signals from the underlying mesenchyme at around E13.5. At approximately E16.5, the primary bud epithelium proliferates and elongates into the developing fat pad forming a rudimentary tree. Development is arrested at this point until puberty. At puberty, terminal end buds (TEBs) form at the leading edge of the duct and are the site of active proliferation and apoptosis (Dulbecco et al., 1982; Humphreys et al., 1996). The TEB consists of bipotent cap cells that generate both cytokeratin 18 (K18) positive luminal and K14 positive myoepithelial cells. The latter remain in contact with the extracellular matrix (ECM) while the luminal cells polarize with their apical aspect oriented towards the lumen. In the TEB, proliferation creates excess body cells, which generate the mass of the duct as it elongates and a subset of these cells undergoes apoptosis to form the lumen. Clearing of excess cells is complete and the mature ductal structure can be seen beginning at the shoulder of the TEB (Humphreys et al., 1996). A mature duct consists of a layer, one to two cells wide, of K18 positive luminal cells and a single cell layer of K14 positive myoepithelial basal cells. Once the ducts reach the edges of the fat pad, TEBs are reabsorbed and elongation ceases. Concomitant with elongation, the ductal tree is further elaborated by a tightly regulated process of secondary and tertiary branching.

The dynamic changes seen in the MG are regulated by morphogens (Jardé and Dale, 2012; Schwertfeger, 2009), cytokines/growth factors (McNally and Martin, 2011; Watson et al., 2011) and hormones (McNally and Martin, 2011). Integration and regulation of these signals is required for the proper establishment of the MG anlagen and subsequent development through puberty and pregnancy. Past studies have suggested that BMP 2 and 4 play a role during MG development, including bud formation, epithelial mesenchymal communication, proliferation and lumen formation (Hens et al., 2007; Montesano, 2007; Phippard et al., 1996; van Genderen et al., 1994), but understanding of the regulation of BMP signaling during MG development is limited.

The BMP specific intracellular signal transducers of BMPs are SMAD1/5/8 proteins, which become phosphorylated upon binding of BMPs (BMP 2, 4, 6 or 7 among others) to their receptors (BMPR1A, BMPR1B and BMPR2). This binding can be facilitated by cross-veinless 2 (CV2) (Zhang et al., 2010) or other receptor complex proteins. Phosphorylated pSMAD1/5/8 binds SMAD4 and translocates to the nucleus where the complex acts as a transcription factor (Massague et al., 2005; Miyazono et al., 2005). In the extracellular space, availability of BMPs for binding to their receptors is regulated by the secreted proteins Chordin (CHRD), Chordin-like 1 (CHRDL1), Chordin-like 2 (CHRDL2), Noggin (NOG) and TWSG1 among others (Balemans and Van Hul, 2002). While CHRD and NOG are antagonists of BMP action, TWSG1 has a dual role, acting as either a BMP antagonist or as an agonist (Oelgeschlager et al., 2000; Ross et al., 2001) which has been shown in *Danio rerio*, *Drosophila* and *Xenopus* (Little and Mullins, 2004; Oelgeschlager et al., 2000; Shimmi et al., 2005). CHRD can be cleaved by the matrix metalloproteinase (MMP) BMP1, also known as tolloid, which can release ligand into the extracellular space. Cleavage of Chordin by BMP1 is enhanced when TWSG1 participates in the complex of Chordin and BMP (Xie and Fisher, 2005).

Mice deficient for TWSG1 have a number of developmental defects, including craniofacial malformations (Billington et al., 2011b; MacKenzie et al., 2009; Zakin and De Robertis, 2004), defects of the vertebrae, kidneys, thymus (Nosaka et al., 2003), and other organs that require branching morphogenesis such as salivary glands (Melnick et al., 2006). Given the role of TWSG1 in the development of branched organs, the goal of this study was to understand the role of TWSG1 during postnatal ductal maturation in the MG and to determine how perturbations in BMP signaling may affect that maturation.

Materials and methods

Mice

Generation and genotyping of mice deficient for TWSG1 (C57BL/6 background) and heterozygous gene targeted Twsg1/Lac-Z knock-in mice have been previously reported (Gazzerro et al., 2006; Petryk et al., 2004). Use and care of the mice in this study were approved by the University of Minnesota Institutional Animal Care and Use Committee.

Whole mount hematoxylin and X-Gal staining, elongation and branching analysis

Inguinal MGs (#4) were harvested from female mice in early puberty (Nelson et al., 1990) (day of vaginal opening, about six weeks of age). Some mice were allowed to recover and the contralateral MG was harvested at 10 weeks and stained as previously described (Li et al., 2002). MGs from 3 wk old females were also collected. Mammary glands that were collected from 10 wk animals were staged for metestrus by vaginal observation and vaginal smears. Briefly, whole glands were fixed in 4% paraformaldehyde (Polysciences, Inc., Warrington, PA) for 2 h on ice, defatted with acetone and stained with hematoxylin (Fischer Scientific, Waltham, MA), cleared with xylenes and the gland flattened between two slides for image capture. For whole-mount lacZ staining, fat pads containing the mammary glands were isolated, fixed in ice-cold 2% formaldehyde, 0.2% gluteraldehyde, 0.01% sodium deoxycholate, 0.02% Nonidet-P40 (NP40) in PBS for 5 min, washed with 2 mM $MgCl_2$ in PBS, and stained in X-gal solution [0.1 M phosphate pH 7.3, 2 mM $MgCl_2$, 0.01% sodium deoxycholate, 0.02% NP40, 5 mM $K_3Fe(CN)_6$, 5 mM $K_4Fe(CN)_6$] supplemented with 1 mg X-Gal (Promega) on a rotating wheel, at room temperature, in the dark and overnight. Following washing in PBS and refixing in 2% formaldehyde, 0.2% gluteraldehyde, the pads where photographed or dehydrated and processed for paraffin embedding and sectioning. The extent of fat pad colonization, secondary branching and TEB area were calculated as previously described (Khialeeva et al., 2011; McCaffrey and Macara, 2009; Richards et al., 2004). Briefly, the length and width of the ductal tree were measured as well as the length and width of the stromal fat pad. Areas were calculated for both, and a ductal tree:fat pad ratio was calculated. The extent of secondary branching was calculated by counting branch points within a 2×3-mm^2 area within 1 mm of the lymph node and TEB area was calculated by using the freehand tool in ImageJ (Rasband, 1997–2011) to trace the TEB, diameter was also calculated using the straight line tool.

Immunohistochemistry

Female mice at the onset of puberty were injected intraperitoneally (30 ng/g bodyweight) with bromo-2′-deoxy-uridine (BrdU) (Roche, Indianapolis, IN) and sacrificed 3 h later. Inguinal MGs (#4) were harvested and fixed in 4% paraformaldehyde on ice for 2 h, embedded in paraffin and sectioned at 5 μM. Sections were deparaffinized in xylenes, rehydrated through a series of graded ethanols. For pSMAD1/5/8, GATA-3, ECAD, K8 and K14 staining, antigen retrieval was performed. Slides were placed in Antigen Unmasking

Solution diluted to manufacturer's recommendation (Vector Laboratories, Burlington, CA) and microwaved for 20 min. Once cooled, slides were washed and then blocked in PBS containing 5% goat serum (Invitrogen, Carlsbad, CA) and 0.3% Triton X-100 (Fisher Scientific) for 60 min at room temperature. Sections were incubated with anti-pSMAD1/5/8 (Cell Signaling Technology Inc., Danvers, MA) 1:50, anti-GATA-3 (BD Pharmigen, San Diego, CA) 1:50, anti-E-Cadherin (Cell Signaling Technology Inc.) 1:100, anti-Keratin-14 (Covance, Princeton, NJ) 1:200, anti-Keratin-18 (TROMA-I) (Developmental Studies Hybridoma Bank, Iowa City, IA) 1:200 or anti-Progesterone receptor (Sigma) 1:50. Sections were developed either with Alexa Fluor (Invitrogen) or DyLight (AbCam, San Francisco, CA) species-appropriate fluorophore conjugated secondary antibodies. Fluorescence was visualized on a Zeiss 710 LSM Confocal Microscope using an Argon12 laser (excitation 488 nm), a HeNe laser (excitation 543 nm) a HeNe laser (excitation 633). Images were taken under identical conditions and post-acquisition manipulations were also identical.

Cell culture

HC11 mouse mammary cells (Danielson et al., 1984) (a gift from Dr. Schwertfeger), derived from pregnant BALB/c mouse MG were cultured in RPMI 1640 medium (ATCC, Manassas, VA) supplemented with 10% fetal calf serum (ATCC), 5 µg/ml insulin (Sigma) and 10 ng/ml epidermal growth factor (Invitrogen). Cells were cultured in a humidified atmosphere of 5% CO_2 in air at 37 °C. Prior to BMP treatment cells were serum starved for 24 h, and then treated with either BSA or recombinant BMP7 50 ng/ml (R&D Systems).

Cell proliferation and apoptosis

BrdU incorporation was visualized using bromo-2′-deoxy-uridine Labeling and Detection Kit II (Roche) following manufacturer's instruction and double stained with anti-K18 (Developmental Studies Hybridoma Bank) 1:200. Five TEBs per section ($n=5$) from five MGs were image captured. The number of BrdU positive cells and the total number of K18 positive cells were counted by two independent scorers who were blinded to genotype and the total number of BrdU positive cells are presented as a fraction of total nuclei. Using the same method, apoptotic cells were visualized with TUNEL staining (Gavrieli et al., 1992) using a DeadEnd Fluorometric TUNEL System (Promega, Madison, WI) following manufacturer's instructions. The total number of TUNEL positive nuclei within a TEB structure was expressed as a percentage of all nuclei within that structure.

cDNA generation, RT-PCR and qRT-PCR

Whole inguinal MGs (#4) were collected from WT and $Twsg1^{-/-}$ virgin female mice at the onset of puberty, lymph node removed, and MG lysed in TRIzol reagent (Invitrogen). Furthermore, inguinal MGs were collected and lysed in TRIzol from WT mice at 3 weeks, 10 weeks and early pregnancy (10.5 days past coitus). After extraction with TRIzol, RNA was isolated using RNeasy micro kit (Qiagen, Germantown, MD) following manufacturer's instructions. A similar procedure was followed to obtain total RNA from HC11 cells. Reverse transcription was carried out with the Thermoscript RT-PCR System (Invitrogen) priming with Oligo (dT)$_{20}$, followed by RT and qRT-PCR (Q-PCR, MX3000p, Agilent, LaJolla, CA) for BMP pathway components. Primers for BMP pathway components have been previously published (Sun et al., 2010). Our approach, given the expected reduced epithelium within the $Twsg1^{-/-}$ gland, was to first calculate a ratio between $Gapdh$ and $K18$ and then use this ratio to normalize the signal of the gene of interest. This allowed us to look both at relative whole gland expression as well as relative epithelial expression.

Western blotting

Whole inguinal MGs were collected from virgin, female mice at the onset of puberty, lymph node removed and lysed in modified RIPA buffer (250 µl of 140 mM NaCl, 0.4 mM Tris–HCl pH 8.0, 1% Glycerol, 1% NP40, 2% BSA with Complete Protease Inhibitor Cocktail (Roche) and PhosSTOP (Roche)). SDS-PAGE was used to separate proteins and separated proteins were transferred to PVDF membrane. The membranes (Invitrogen) were blocked with Odyssey blocking buffer (LI-COR, Lincoln, NE, USA) containing 0.1% v/v Tween 20. Membranes were incubated overnight at 4 °C with anti-p-Smad1/5/8 (Cell Signaling Technology Inc.) 1:250, anti-Total SMAD (Santa Cruz Biotechnology, Santa Cruz, CA) 1:100 and anti-GAPDH (ABCam, Cambridge, MA) 1:5000 antibodies and washed before incubation with species-appropriate fluorescent conjugated secondary antibodies for 1 h at room temperature. After washing to remove trace detergent, membranes were analyzed using an Odyssey Infrared Imaging System (LI-COR; Millennium Science, Surrey Hills, Australia) using the manufacturer's protocol. Relative pSMAD1/5/8 was calculated by first normalizing the signal intensity for total SMAD to GAPDH to control for loading. Then pSMAD1/5/8 signal was expressed as a percentage of the total SMAD pool. To detect GATA-3 membranes were incubated overnight at 4 °C with anti-GATA-3 antibody at 1:50 dilution (AbCam, San Francisco, CA), probed with anti-mouse HRP-conjugated secondary antibody (Cell Signaling Technology Inc.), and visualized with SuperSignal West Pico Chemiluminescent Substrate (Thermo Scientific, Rockford, IL).

Mammary gland transplantation

Mammary glands from 3 wk old $Twsg1^{-/-}$ host females or WT host females were cleared of endogenous epithelium as described (DeOme et al., 1959). Donor mammary tissue was collected from adult wild type (WT) and $Twsg1^{-/-}$ mice and minced into small fragments. WT and $Twsg1^{-/-}$ mammary fragments were transplanted into the cleared host fat pads, with each host (both WT and $Twsg1^{-/-}$) mouse receiving a WT transplant and a contralateral $Twsg1^{-/-}$ transplant. Host fat pads containing transplanted epithelium were removed and processed for whole-mount hematoxylin staining as described above. Approximately 80% of all transplants were able to colonize and elongate into the host fat pad.

Statistical analyses

Gene expression levels were normalized to K18/GAPDH and significance calculated using a Student's t-test with significance set at $p < 0.05$. pSMAD signal intensity was normalized to total SMAD which was first normalized to GAPDH. Significance was calculated using a Student's t-test with significance set at $p < 0.05$.

Results

TWSG1 and other BMP signaling pathway components are present in the mammary gland during postnatal development

To determine the presence and timing of TWSG1 expression during MG postnatal development, LacZ staining of mammary glands from heterozygous mice with LacZ inserted into the $Twsg1$ locus and RT-PCR for BMP pathway components was performed. $Twsg1$ was detected by LacZ staining in the myoepithelium and in a subset of body cells within the canalizing TEB (Fig. 1A and B) at 6 weeks. In the mature gland, $Twsg1$ was expressed throughout the ductal tree and was primarily expressed in the myoepithelium (Fig. 1C and D). Given that TWSG1 modulates BMP signaling, components of the BMP pathway were assessed by RT-PCR across
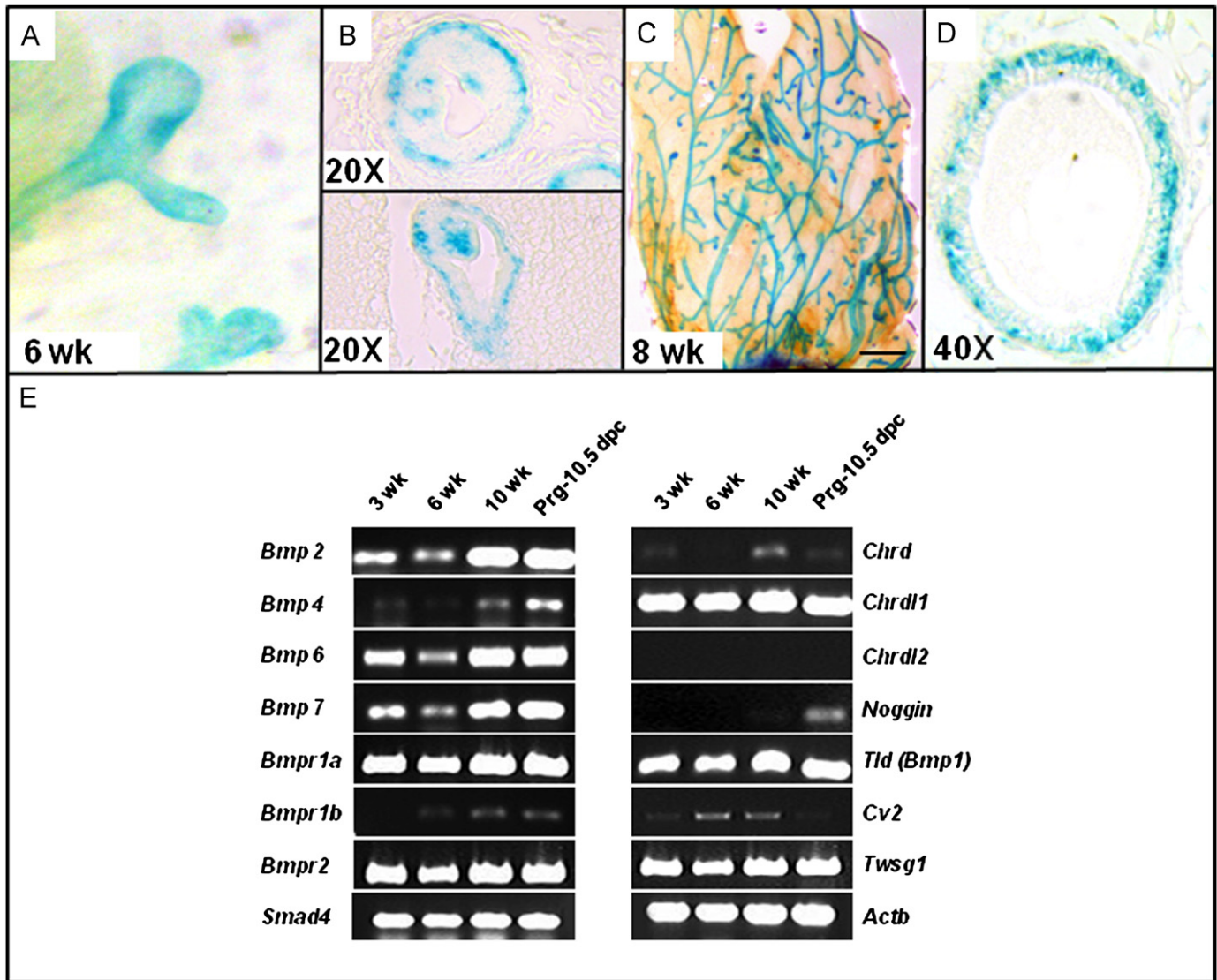
Fig. 1. *Twsg1* and BMP pathway components are expressed in the mammary gland (MG) at important postnatal developmental time points. (A–D) LacZ staining of whole mount (A and C) and sectioned (B and D) mammary glands isolated from heterozygous 6 and 8 wk old virgin female carrying *LacZ* reporter gene in the *Twsg1* locus. (A) *Twsg1* is present in ducts and terminal end buds (TEBs) at 6 weeks (B) and in a subset of body cells in the canalizing TEB. (C) *Twsg1* expression is present in the mature ducts (2 mm scale bar). (D) This expression is observed primarily in the myoepithelium at 8 weeks. (E) RT-PCR showing temporal expression of BMP pathway members in MGs at different postnatal developmental time points. *Actb*, beta-actin, *Chrd*, chordin; *Chrdl1*, chordin-like 1; *Chrdl2*, chordin-like 2; *Cv2*, crossveinless 2.

developmentally relevant time points (Fig. 1E). mRNA for *Bmp1*, *Bmp2*, *Bmp6*, *Bmp7*, *Bmpr1a*, *Bmpr2*, and *Smad4* were expressed across all time points. The Type1 receptor *Bmpr1b* was barely detectable. *Bmp4* was detected at 10 weeks and at pregnancy. Among genes encoding BMP-binding proteins, *Twsg1* mRNA was expressed at all time points while others were more temporally expressed. Chordin (*Chrd*) was undetectable at 6 weeks and barely detectable at other stages, while Chordin-like 1 (*Chrdl1*) was strongly expressed at each time point. Noggin (*Nog*) was expressed only during pregnancy while Chordin-like 2 (*Chrdl2*) was undetectable (Fig. S1). *Cv2* mRNA was not detected during pregnancy, but was present at other time points.

TWSG1 is required for timely ductal elongation and fat pad colonization

MGs from WT and *Twsg1*$^{-/-}$ female mice were examined at 3, 6 and 10 weeks. The ductal trees were comparable at 3 weeks with the establishment of a rudimentary tree (Fig. 2A and D) although TEBs appeared atypical in the *Twsg1*$^{-/-}$ MG (Fig. 2G).

At 3 weeks, TEBs were smaller than WT and in some cases it appeared as if TEBs were not established. At 6 weeks, the WT ducts had elongated well past the lymph node (LN) while the *Twsg1*$^{-/-}$ ducts showed little elongation. In most cases, the ducts did not reach or just reached the LN (Fig. 2B and E). The TEBs in the *Twsg1*$^{-/-}$ were larger than WT TEBs at this time point (Fig. 2H). At 10 weeks, the WT ducts had completely elongated, were well branched and the TEBs had reabsorbed. In *Twsg1*$^{-/-}$ ducts, TEBs were still present and the ductal tree was not as robustly branched (Fig. 2C and F). At 10 weeks, the WT TEBs had reabsorbed while TEBs were still found in the *Twsg1*$^{-/-}$ MG (Fig. 2I). A reduction in secondary branching in *Twsg1*$^{-/-}$ MGs at 10 weeks was also observed. The most striking difference between WT and *Twsg1*$^{-/-}$ ductal morphogenesis was found at 6 weeks and this stage was assessed further.

TWSG1 is required for timely elongation and fat pad colonization

MGs from *Twsg1*$^{-/-}$ female mice were examined on the first day of vaginal opening, approximately 6 weeks of age. MGs from WT
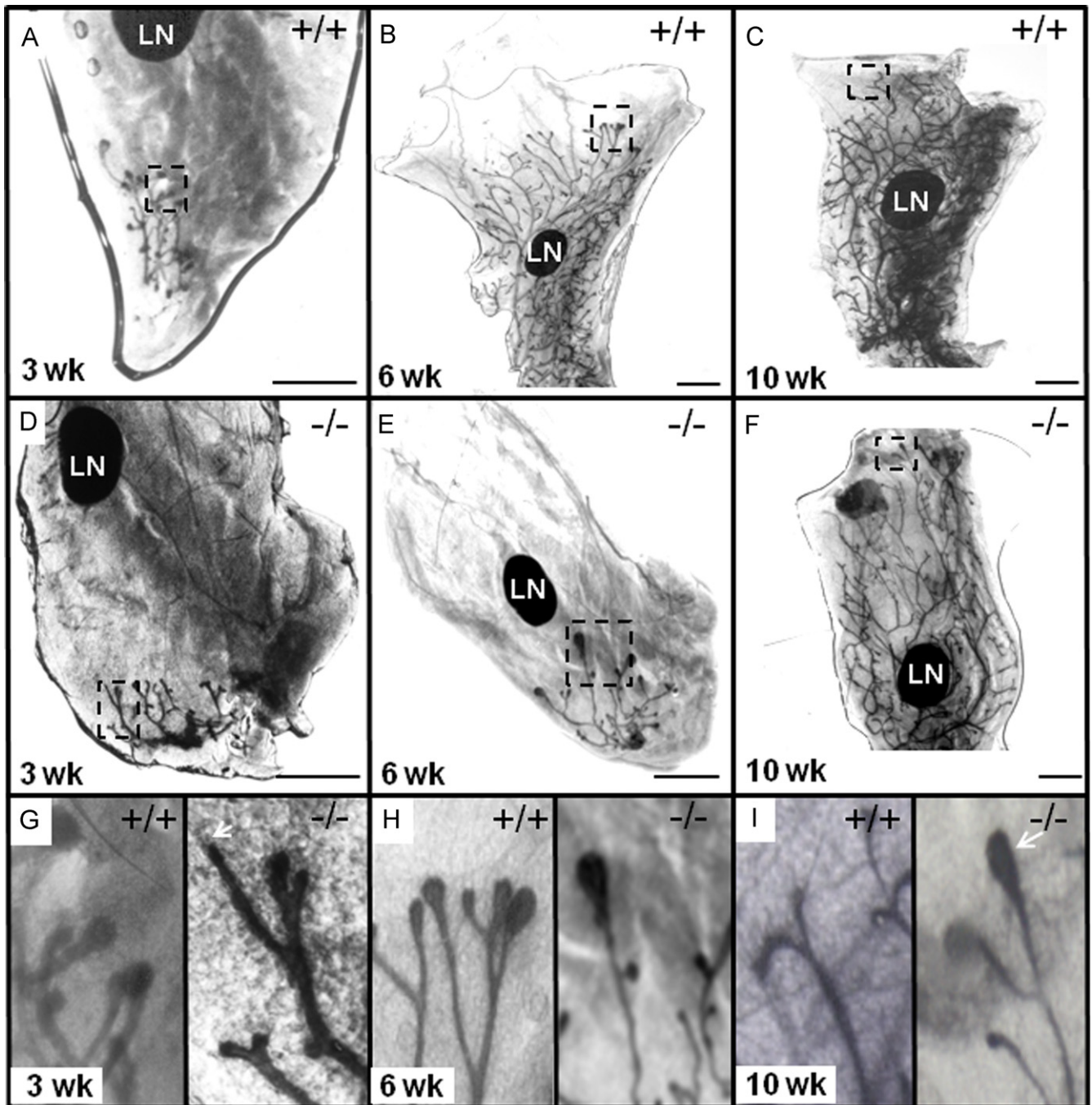
Fig. 2. Loss of TWSG1 results in a delay of ductal elongation. (A, B, C) Whole mount MG from 3, 6 and 10 wk old wild type (WT) virgin female mouse. (D, E, F) Whole mount MG from 3, 6 and 10 wk old $Twsg1^{-/-}$ virgin female mouse. (G, H, I) Distal ends of ductal tree from the MG of 3, 6 and 10 wk WT and $Twsg1^{-/-}$ virgin female mouse. Arrow indicates poorly formed TEB (2G) and TEBs still present at 10 weeks (2I) in the $Twsg1^{-/-}$ MG. Magnified distal ends are boxed. LN, lymph node. Scale bar 2 mm.

animals contained ducts that extended past the lymph node and were robustly branched. In contrast, $Twsg1^{-/-}$ mice showed a significant decrease in fat pad colonization (Fig. 3A) with 38% of fat pad being occupied by the ductal network in $Twsg1^{-/-}$ MGs ($n=5$) compared to 64% in WT MGs ($n=5$, $p=0.0032$) at 6 weeks of age. In addition, secondary branching was significantly reduced in MGs from 6 wk old virgin $Twsg1^{-/-}$ animals compared to WT (Fig. 3B) and TEBs were significantly larger in $Twsg1^{-/-}$ ducts (Fig. 3C).

Delay in elongation is intrinsic to the MG

To determine if the delay in ductal elongation and fat pad colonization was intrinsic to the MG rather than secondary

to other factors, for example alterations in hormonal milieu, we performed transplantation experiments. We transplanted $Twsg1^{-/-}$ epithelium into the fat pads, cleared of endogenous epithelium, of 3 wk old WT animals. The MGs were analyzed 3 weeks later and there was either a significant delay ($n=2$) or no measurable outgrowth ($n=1$) of $Twsg1^{-/-}$ MG tissue when compared to contralaterally transplanted WT tissue (Fig. 4 A and B). Conversely, WT MG tissue transplanted into the cleared fat pad of $Twsg1^{-/-}$ had outgrowth that was similar to WT tissue transplanted into WT fat pad (data not shown). The TEBs in the $Twsg1^{-/-}$ transplanted tissue were similar in morphology to TEBs in 3 wk $Twsg1^{-/-}$ MGs (Fig. 4C and D).
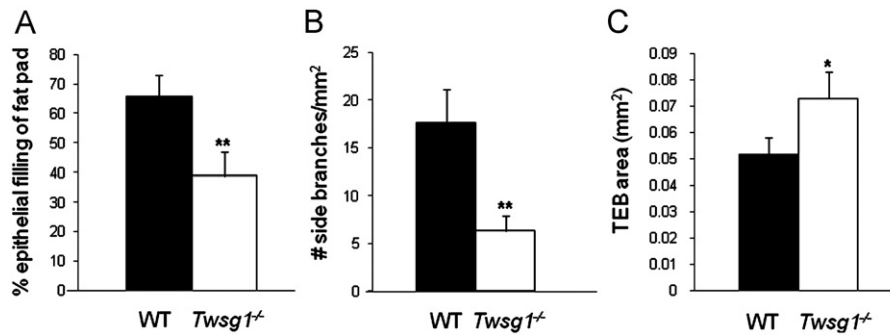
Fig. 3. Loss of TWSG1 results in impaired ductal elongation, reduced secondary branching and enlarged terminal end buds. (A) Percetage of fat pad colonization by the ductal tree in WT and $Twsg1^{-/-}$ virgin female mouse. (B) Side branching is significantly reduced in $Twsg1^{-/-}$ MG. (C) TEBs are significantly larger in $Twsg1^{-/-}$ MGs at 6 weeks. **$p < 0.001$.
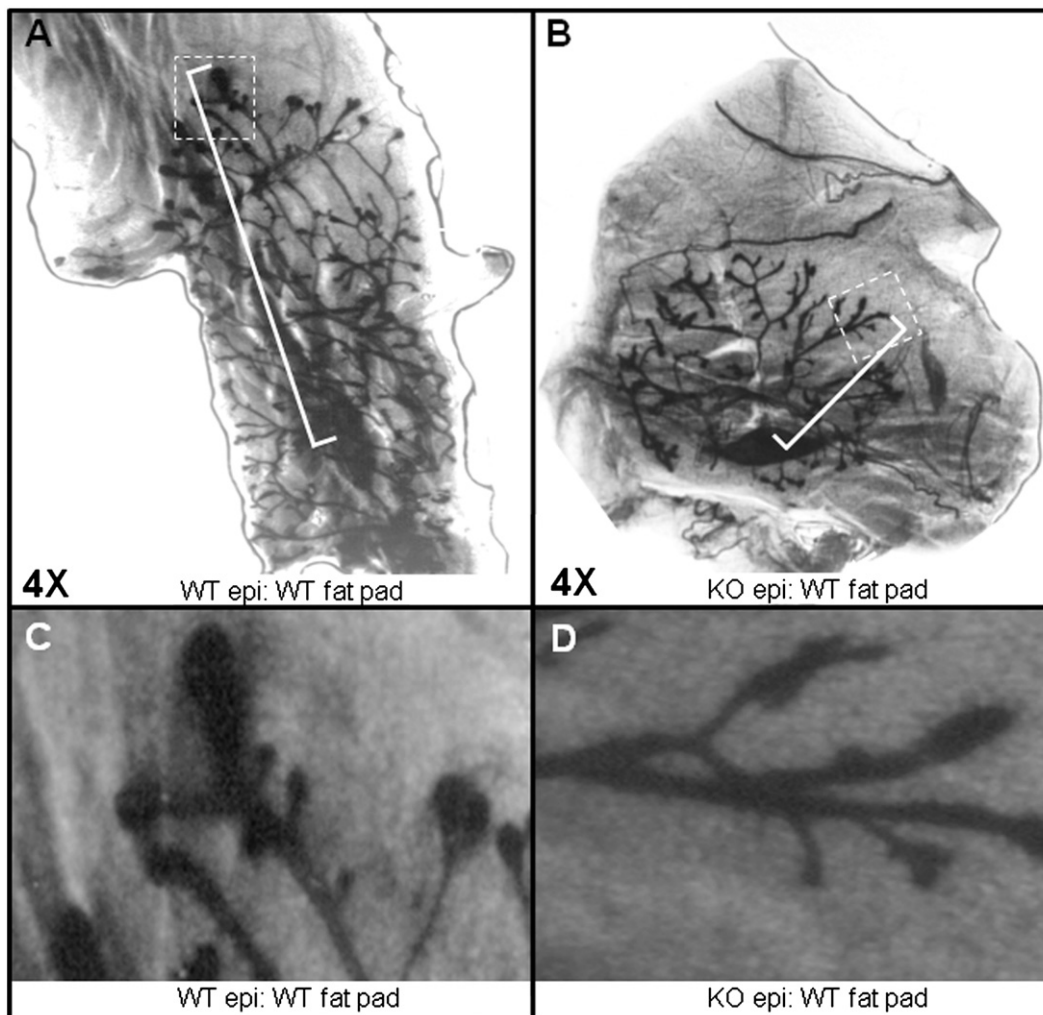

Fig. 4. Elongation defect is intrinsic to the MG. (A) WT epithelium transplanted into cleared fat pad of 3 wk old WT mouse shows adequate elongation ($n=3$) as measured from center of transplanted epithelium to distal end of longest primary duct. Longest primary duct is bracketed and farthest distal end is boxed. (B) $Twsg1^{-/-}$ epithelium transplanted into cleared fat pad of 3 wk old WT mouse shows impaired elongation ($n=3$) as measured from center of transplanted epithelium to distal end of longest primary duct. Longest primary duct is bracketed and farthest distal end is boxed. (C) Magnified view of transplanted WT distal ends. (D) Magnified view of transplanted $Twsg1^{-/-}$ distal ends.

BMP signaling is reduced in the MG epithelium

To further investigate BMP signaling within the $Twsg1^{-/-}$ MG, a western blot was performed to detect pSMAD1/5/8. BMP signaling via pSMAD was significantly reduced in the $Twsg1^{-/-}$ MG (Fig. 5A).

Co-localization studies demonstrated that in the WT MG pSMAD1/5/8 was localized to nuclei of cells within the TEB and pSMAD1/5/8 signal could not be detected in the $Twsg1^{-/-}$ TEB (Fig. 5B). We also observed that BMP downstream targets, *Msx1*, *Msx2* and *Gata-3*, were downregulated in $Twsg1^{-/-}$ MG (Fig. 5C).
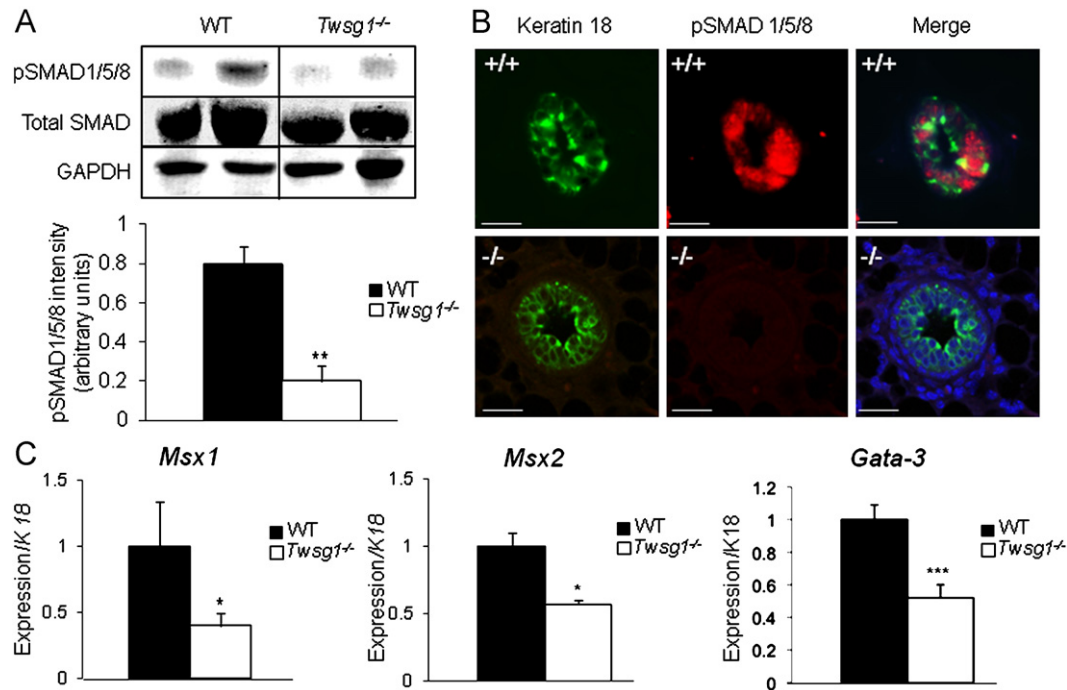
Fig. 5. BMP signaling is reduced in MGs from $Twsg1^{-/-}$ animals. (A) Western blot, showing two representative samples per group, detecting the levels of total SMAD, pSMAD1/5/8 and GAPDH in MG lysates from WT and $Twsg1^{-/-}$ 6 wk old virgins. Total SMAD was normalized to GAPDH and a ratio of SMAD to pSMAD1/5/8 was calculated; $p < 0.002$. (B) Immunofluorescence staining for epithelial marker keratin 18 (green) and pSMAD1/5/8 (red). pSMAD1/5/8 is absent in $Twsg1^{-/-}$ MGs. (C) Q-PCR for BMP downstream targets, Msx1, Msx2 and Gata3, shows reduced expression in $Twsg1^{-/-}$ MGs. Scale bar 2 um.

TWSG1 mediates lumen formation and luminal identity

Whole mount light microscopy of $Twsg1^{-/-}$ MGs showed a density of staining in the duct that was suggestive of a difference in cell density between WT and $Twsg1^{-/-}$ MGs. To investigate this further we sectioned MGs from 6 wk old virgin females and stained with K18, K14 and Trichrome and assessed mature ducts. WT MGs at 6 weeks had mature ducts with a clear, well-defined lumen (Fig. 6A–C, G–I, M and N) with no cells visible within the lumen. Conversely, the $Twsg1^{-/-}$ MGs contained a mix of ducts containing cell islets (Fig. 6D–F), completely occluded ducts (Fig. 6J–L) as well as single cells shed into the lumen (Fig. 6Q and R) and clear lumens. Approximately 60% of the mature ducts in the $Twsg1^{-/-}$ MG had either complete or partial occlusion. When occluded ducts were stained for K14, the cells within the lumens contained an organized structure that consisted of a secondary K14 positive compartment surrounding a mass of K14 negative cells (Fig. 6D–F). This "duct within a duct" structure was only observed in $Twsg1^{-/-}$ MGs. WT, mature ducts consisted of a clearly defined luminal compartment that was K18 positive (Fig. 6G–I). Using a blood vessel landmark, the luminal compartments of $Twsg1^{-/-}$ ducts were further examined. In many cases, the duct remained occluded until out of the plane of sectioning and not all cells within the occlusion were K18 positive (arrows) (Fig. 6J–L). To look more closely at $Twsg1^{-/-}$ myoepithelial compartment, K14 stained sections were interrogated for the presence of basal body cells, which are K14 positive cells within the luminal compartment. In WT ducts, no basal body cells were observed (Fig. 6M and N), consistent with previous reports (Mailleux et al., 2007). Within $Twsg1^{-/-}$ MGs ~60% of the ducts observed contained K14 positive basal body cells. To further characterize the cells within the luminal compartment ducts were stained for smooth muscle actin (SMA) and a similar distribution of SMA positive cells were seen in the $Twsg1^{-/-}$ MG (data not shown). Additionally, we observed cell shedding in

$Twsg1^{-/-}$ but not WT mature ducts. Usually these were single or small groups of cells within the lumens of mature ducts and these shed cells were K14 positive (Fig. 6Q and R).

Apoptotic defect may lead to accumulation of cells and poor lumen formation in Twsg1 mutant ducts

The TEBs of MGs from $Twsg1^{-/-}$ animals are larger than WT controls suggesting hyperplasia. To assess this further we counted the number of cells within TEB structures (five animals, five sections per animal) in WT and $Twsg1^{-/-}$ MGs. There was a significant increase in the number of K18 positive cells within the $Twsg1^{-/-}$ TEBs (Fig. 7A). To determine if this was due to an increase in proliferation or a decrease in apoptosis we stained for BrdU and performed a TUNEL assay. BrdU incorporation revealed no significant difference in proliferation between WT and $Twsg1^{-/-}$ TEBs (Fig. 7B and D). To determine if known regulators of proliferation are changed in our model, we assessed the expression of insulin-like growth factor 1, amphiregulin and estrogen receptor alpha by Q-PCR. There were no significant differences detected (data not shown). Furthermore, amphiregulin and progesterone receptor were visualized by IF and no differences in distribution were observed (data not shown). However, there was a marked decrease of nearly four-fold in apoptosis within the $Twsg1^{-/-}$ TEBs (Fig. 7C and D).

TWSG1 plays a role in restricting K14 positive cells to the basal compartment

Gata-3 is required for luminal identity in the MG and is a downstream target of BMP signaling in various tissues (Bonilla-Claudio et al., 2012). In WT TEBs (Fig. 8A–D) and mature ducts (Fig. 8I–L) almost all luminal cells expressed GATA-3. In contrast, $Twsg1^{-/-}$ MGs consisted of TEBs (Fig. 8E–H) and mature ducts (Fig. 8M–P) that were a mosaic of GATA-3 positive and
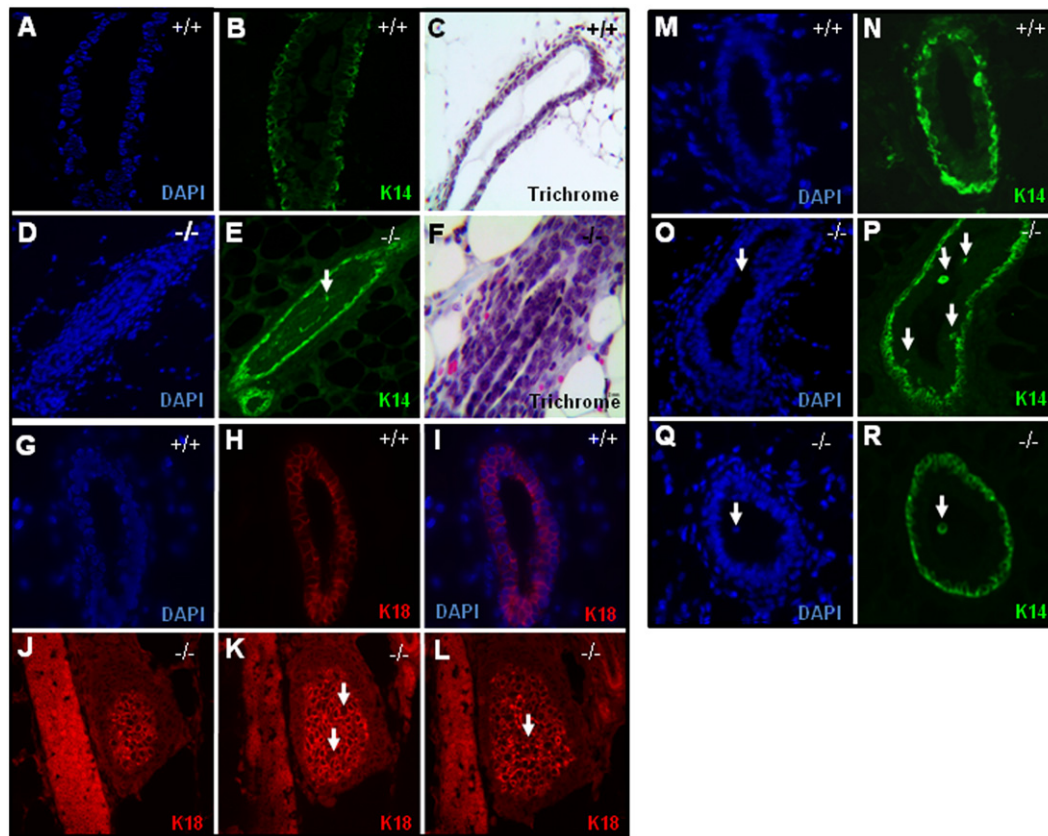
Fig. 6. $Twsg1^{-/-}$ MGs have abnormal epithelial organization, occluded lumens and cell shedding at puberty. (A–C) WT MGs (D–F) $Twsg1^{-/-}$ MGs stained with K14 have occluded lumens, which can be organized with a secondary myoepithelial compartment surrounding a mass of K14 negative cells. (C and F) Trichrome staining reveals cleared lumens of WT ducts and an organized cell mass within some lumens of the $Twsg1^{-/-}$ maturing duct. (G–I) WT ducts with a well formed lumen. (J–L) Using a blood vessel to mark the location within the MG, serial sections of an occluded $Twsg1^{-/-}$ duct were stained for K18. Not all the cells that occlude the lumen are K18 positive (arrows). (M and N) K14 stained WT mature ducts showing K14 positive cells in the basal compartment, but not the luminal compartment of the epithelium at puberty. (O and P) K14 positive cells are found in the luminal compartment of $Twsg1^{-/-}$ mature ducts (arrow). (Q and R) Cell shedding in $Twsg1^{-/-}$ ducts. Cells shed into the lumen were preferentially K14 positive. All images were taken at $20 \times$.
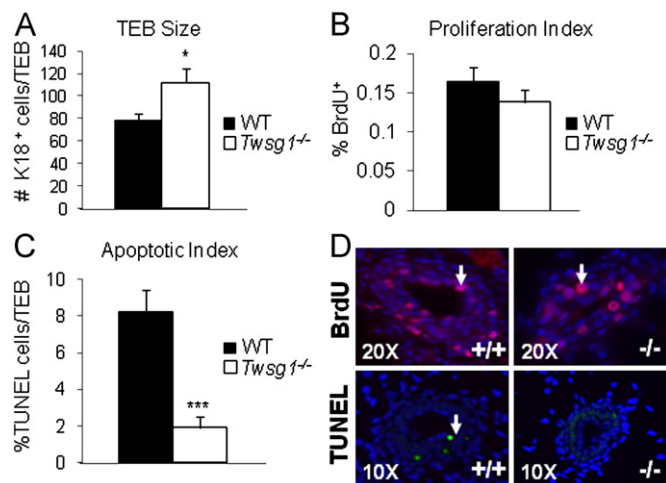

Fig. 7. $Twsg1^{-/-}$ TEBs show an increase in luminal epithelial (K18) cell number and a decrease in apoptosis. (A) K18 positive cells were counted within TEBs and compared between WT and $Twsg1^{-/-}$. A significant increase in cell number was observed in $Twsg1^{-/-}$ compared to WT. (B) BrdU positive cells were counted within the same compartment and no significant change in proliferation was observed. (C) TUNEL staining revealed a significant decrease in the number of apoptotic cells within the TEB of $Twsg1^{-/-}$ MGs. (D) Representative images for BrdU (pink), K18 (green) and TUNEL (green) staining. $^{*}p < 0.05$, $^{***}p < 0.001$.

GATA-3 negative cells. In $Twsg1^{-/-}$ MGs, single cells that were shed into the lumen were GATA-3 negative (Fig. 8P). To confirm that BMPs could induce $Gata$-3 expression in mammary epithelial cells, HC11 cells were treated with BMP7 50 ng/ml and $Gata$-3 mRNA expression measured by Q-PCR. BMP7 induced $Gata$-3 expression over two-fold ($p=0.0004$) (Fig. 9A). We also assessed $Gata$-3 expression and protein content and found that $Gata$-3 expression (Fig. 9B) as well as protein level (Fig. 9C) were reduced in $Twsg1^{-/-}$ MGs.

Discussion

TWSG1 as a positive regulator of BMP signaling during postnatal MG development

Studies in *Drosophila melanogaster*, *Danio rerio*, *Xenopus*, and *Mus musculus* have shown that TWSG1 is a highly conserved extracellular modulator of BMP signaling with important roles during embryonic development (Ross et al., 2001; Scott et al., 2001; Zusman and Wieschaus, 1985). Recent studies have demonstrated that TWSG1 continues to be an important BMP regulator in adult mammalian tissues, including bone homeostasis (Sotillo Rodriguez et al., 2009), regeneration following ischemic kidney injury (Larman et al., 2009), immune responses (Tsalavos et al., 2011), and, as this study shows, postnatal MG ductal maturation.
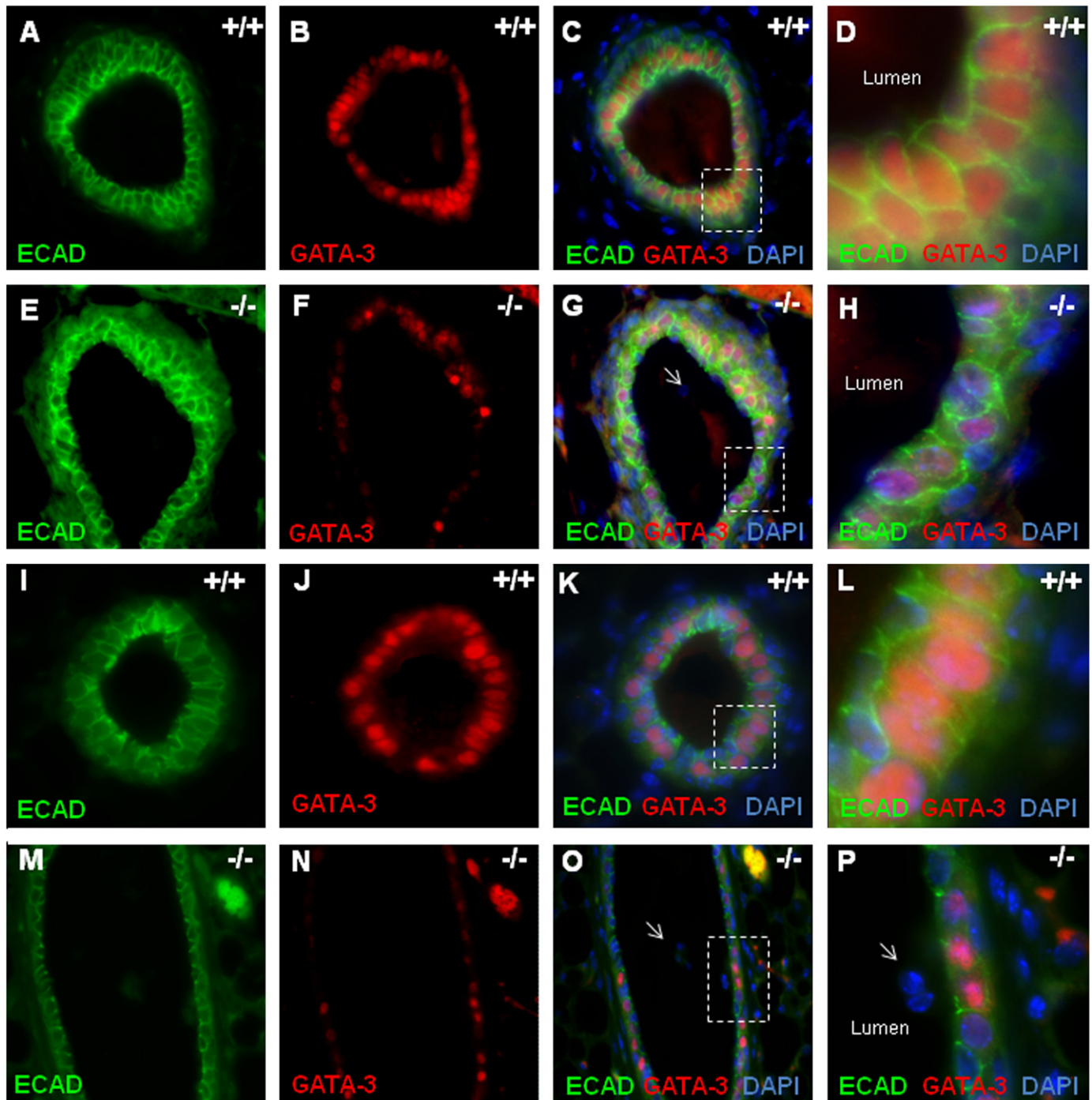
Fig. 8. GATA-3, required for luminal identity, is reduced in *Twsg1*$^{-/-}$ MGs. GATA-3 expression is reduced in *Twsg1*$^{-/-}$ MGs. ECAD was used to mark luminal epithelial cells and most ECAD positive cells in the WT TEB express GATA-3 (A–D) and mature duct (I–L) while the *Twsg1*$^{-/-}$ TEB (E–H) and mature duct (I–L) consist of a mosaic of GATA-3 positive and GATA-3 negative luminal cells. Most cells shed into the lumen are GATA-3 negative (P). All images were taken at 40×. Boxes in C, G, K, and O correspond to the magnified images in D, H, L, and P, respectively.

It is known that TWSG1 interacts with BMP2, BMP4, and BMP7 (Billington et al., 2011a; Blitz et al., 2003; Chang et al., 2001; Ross et al., 2001; Scott et al., 2001), either directly or by forming complexes with CHRD (Larrain et al., 2001). While in *Xenopus* and *Denio rario* TWSG1 can act as a BMP antagonist as well as an agonist (Blitz et al., 2003; Ross et al., 2001; Xie and Fisher, 2005), the latter function has not been directly demonstrated in mammals. In this study, BMP signaling is reduced in the murine MG in the absence of TWSG1, suggesting pro-BMP activity in the postnatal MG. It is thought that the pro-BMP activity of TWSG1 results from its ability

to facilitate the cleavage of CHRD by the MMP BMP1 in the extracellular space (Larrain et al., 2001). *Chrd* was not detected in the MG at 6 weeks, suggesting that CHRD-independent mechanisms may play a role (Xie and Fisher, 2005) A potential binding partner is CHRDL1, which is highly expressed in the developing MG and has been shown to bind BMPs and TWSG1. Intriguingly, in cells of the proximal tubule of the kidney, CHRDL1 amplifies BMP4 signaling in the presence of TWSG1 (Larman et al., 2009).

Reduced expression of the BMP targets *Msx1*, *Msx2*, *Gata-3*, and decreased levels of pSMAD1/5/8 all indicate a reduction of BMP
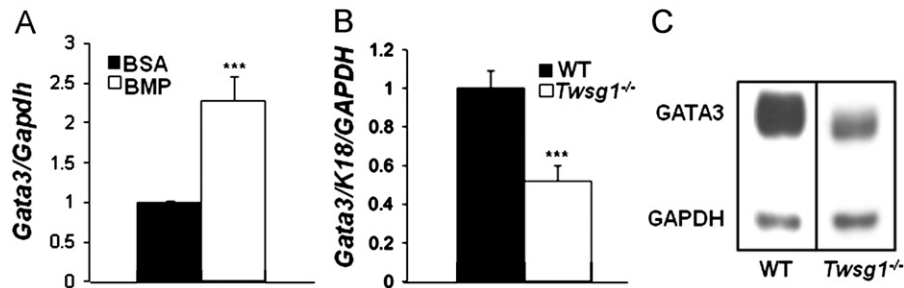
Fig. 9. GATA-3, required for luminal identity, is reduced in $Twsg1^{-/-}$ MGs. (A) $Gata-3$ expression is significantly upregulated in HC11 cells that have been treated with BMP7 (50 ng/ml). (B) $Gata-3$ expression is significantly downregulated, in $Twsg1^{-/-}$ MGs from 6 wk old virgin mice. (C) There is reduced GATA-3 protein in $Twsg1^{-/-}$ MGs ($n=3$) compared to WT ($n=3$).

signaling in the $Twsg1^{-/-}$ MG. Mutations in $Msx1$ and $Msx2$ result in impaired MG development. MGs of $Msx2$-deficient mice arrest at the mammary sprout stage while the epithelium of the $Msx1/Msx2$ double-deficient mice fails to form a bud with subsequent regression of the MG anlagen (Satokata et al., 2000). $Bmp2$ and $Bmp4$ mutants are embryonic lethal (Lawson et al., 1999; Zhang and Bradley, 1996) and no studies have specifically addressed the effects of deletion of these genes in the postnatal MG. Thus, the $Twsg1^{-/-}$ mouse provides a model in which to evaluate the consequences of perturbated BMP signaling during postnatal ductal maturation.

TWSG1 is essential for postnatal ductal maturation in the murine MG

Postnatal MG development is orchestrated by numerous hormones, growth factors, cytokines, and transcription factors including MSX1, MSX2 and GATA-3, which regulate proliferation, apoptosis, and differentiation (McNally and Martin, 2011). Although BMPs are known to regulate proliferation through $Msx1$ (Zhang et al., 2002) and the expression of $Msx1$ was decreased in the $Twsg1^{-/-}$ MG, proliferation was not significantly altered suggesting that other pathways are involved in regulating proliferation in the elongating duct. In contrast, apoptosis was reduced in $Twsg1^{-/-}$ MG, indicating a role for BMP-induced apoptosis in lumen formation. Furthermore, $Twsg1$ is expressed in a subset of body cells within the TEB making it available for regulation of BMP signaling within the canalizing TEB. The classical mediator of the pro-apoptotic effects of BMPs is $Msx2$ (Graham et al., 1996). Indeed, reduced $Msx2$ expression was seen in the $Twsg1^{-/-}$ MG. The reduced apoptosis in the TEB could explain the observation that 60% of the mature ducts in the $Twsg1^{-/-}$ MG were occluded or had cell islets present in the lumen. It has been shown that disrupted apoptosis can be accompanied by lumen filling and cell shedding in the MG (Mailleux et al., 2007). However, it is also possible that cells shed into the lumen repopulate the lumen with a mass of cells that is later cleared by some unknown mechanism.

GATA-3 is directly induced by BMP signaling during facial skeletal development (Bonilla-Claudio et al., 2012), preplacodal ectoderm specification (Kwon et al., 2010), and hair follicle morphogenesis (Kobielak et al., 2003). In the MG, GATA-3 deficiency results in impaired placode formation, elongation defect as a result of the failure of TEBs to stably form, and a reduction in side branching (Asselin-Labat et al., 2007). Additionally, GATA-3 can induce apoptosis in a luminal tumor model (Kouros-Mehr et al., 2008) and upregulate pro-apoptotic genes such as caspase-14 (Asselin-Labat et al., 2011). In mice with MG specific GATA-3 deficiency lumens are irregular and cell shedding is observed (Asselin-Labat et al., 2007). In the $Twsg1^{-/-}$ MG, loss of TWSG1 reduces BMP signaling perhaps by reducing BMP availability. As a result, not all cells reach the BMP signaling threshold required for

$Gata-3$ induction and subsequent adoption of a luminal cell fate. The cells that fail to induce $Gata-3$ will remain in the luminal compartment or be shed into the lumen. It is possible that this mosaic of cell types in the advancing duct inhibits elongation but as cells are lost into the lumen cell:cell contacts are reestablished and elongation can again proceed in the absence of $Twsg1^{-/-}$.

We also observed a decrease in secondary branching in $Twsg1^{-/-}$ MG. As the ducts invade into the fat pad, secondary branching occurs in areas where there is low TGFβ expression (Pierce et al., 1993) and high $Msx2$ expression (Satoh et al., 2004). A recent study demonstrated that BMP2/4 can induce branching in the MG via $Msx2$ upregulation (Fleming et al.). When $Twsg1$ is deleted, some cells receive adequate BMP while others do not and in those regions with reduced BMP, $Msx2$ expression is also reduced and branching is not initiated, thus leading to an overall reduction in secondary branching in the $Twsg1^{-/-}$ MG.

Contribution of TWSG1 to maintaining basal vs. luminal epithelial identity

The MG epithelium is composed of the basal myoepithelial cells and polarized luminal epithelial cells. It is thought that the different cell populations arise from multipotent progenitors, or mammary stem cells (Stingl et al., 1998). Interestingly, in $Twsg1^{-/-}$ MG, K14 positive cells are present within the luminal compartment among K18 positive cells. This suggests that BMP signaling plays a role in establishing and/or maintaining epithelial identity as opposed to myoepithelial, for example through GATA-3 (Metallo et al., 2008; Wilson and Hemmati-Brivanlou, 1995). In $Twsg1^{-/-}$ MGs, the K14 positive cells within the luminal compartment may represent those cells whose BMP exposure was not sufficient to induce $Gata-3$ expression preventing progression towards a terminal luminal fate. In line with this, cells shed into the lumen of $Twsg1^{-/-}$ MGs are K14 positive whereas a previous study demonstrated that deleting $Gata-3$ after luminal specification did not reduce K18 expression showing that GATA-3 is not required for maintenance of K18, only its induction (Kouros-Mehr et al., 2006). This suggests that TWSG1 acts upstream of GATA-3 for regulating epithelial/myoepithelial cell fate.

In summary, this study sheds light on the role of the extracellular regulation of BMP signaling by TWSG1 during postnatal MG development. It shows that BMP signaling is reduced in MG leading to a decrease in $Msx2$ and $Gata-3$ expression. In the absence of TWSG1, delayed ductal elongation, impaired branching and lumen formation, incomplete myoepithelial restriction, and shedding into the lumen are observed. Understanding how TWSG1 regulates normal ductal maturation can provide insight into what role it may be playing during carcinogenesis, especially in light of the recent data suggesting tumor suppressor effects of BMPs (Loh et al., 2008; Owens et al., 2012; Ye et al., 2009).

There is some evidence that the expression of *Bmps*, *Msx2*, and *Twsg1* is altered in breast cancer (Finak et al., 2008; Malewski et al., 2005; Phippard et al., 1996), but the mechanisms for this differential regulation are unknown. Future studies will further elucidate the mechanism by which the lumens are eventually cleared in the absence of TWSG1. This may provide insight into how cells within the MG that escape targeted apoptosis at one point in development are identified and eventually cleared from the MG.

Acknowledgments

Appendix A. Supplementary Information

Supplementary data associated with this article can be found in the online version at http://dx.doi.org/10.1016/j.ydbio.2012.10.007.

References

Asselin-Labat, M.-L., Sutherland, K.D., Vaillant, F., Gyorki, D.E., Wu, D., Holroyd, S., Breslin, K., Ward, T., Shi, W., Bath, M.L., Deb, S., Fox, S.B., Smyth, G.K., Lindeman, G.J., Visvader, J.E., 2011. Gata-3 negatively regulates the tumor-initiating capacity of mammary luminal progenitor cells and targets the putative tumor suppressor caspase-14. Mol. Cell. Biol.. (MCB.05766-11).

Asselin-Labat, M.L., Sutherland, K.D., Barker, H., Thomas, R., Shackleton, M., Forrest, N.C., Hartley, L., Robb, L., Grosveld, F.G., van der Wees, J., Lindeman, G.J., Visvader, J.E., 2007. Gata-3 is an essential regulator of mammary-gland morphogenesis and luminal-cell differentiation. Nat. Cell Biol. 9, 201–209.

Bailey, J.M., Singh, P.K., Hollingsworth, M.A., 2007. Cancer metastasis facilitated by developmental pathways: sonic hedgehog, notch, and bone morphogenic proteins. J. Cell. Biochem. 102, 829–839.

Balemans, W., Van Hul, W., 2002. Extracellular regulation of BMP signaling in vertebrates: a cocktail of modulators. Dev. Biol. 250, 231–250.

Beppu, H., Mwizerwa, O.N., Beppu, Y., Dattwyler, M.P., Lauwers, G.Y., Bloch, K.D., Goldstein, A.M., 2008. Stromal inactivation of BMPRII leads to colorectal epithelial overgrowth and polyp formation. Oncogene 27, 1063–1070.

Billington Jr., C.J., Fiebig, J.E., Forsman, C.L., Pham, L., Burbach, N., Sun, M., Jaskoll, T., Mansky, K., Gopalakrishnan, R., O'Connor, M.B., Mueller, T.D., Petryk, A., 2011a. Glycosylation of twisted gastrulation is required for BMP binding and activity during craniofacial development. Front. Physiol. 2, 59.

Billington Jr., C.J., Ng, B., Forsman, C., Schmidt, B., Bagchi, A., Symer, D.E., Schotta, G., Gopalakrishnan, R., Sarver, A.L., Petryk, A., 2011b. The molecular and cellular basis of variable craniofacial phenotypes and their genetic rescue in twisted gastrulation mutant mice. Dev. Biol. 355, 21–31.

Blitz, I.L., Cho, K.W., Chang, C., 2003. Twisted gastrulation loss-of-function analyses support its role as a BMP inhibitor during early Xenopus embryogenesis. Development 130, 4975–4988.

Bonilla-Claudio, M., Wang, J., Bai, Y., Klysik, E., Selever, J., Martin, J.F., 2012. BMP signaling regulates a dose-dependent transcriptional program to control facial skeletal development. Development 139, 709–719.

Bowman, A., Nusse, R., 2011. Location, location, location: FoxM1 mediates β-catenin nuclear translocation and promotes glioma tumorigenesis. Cancer Cell 20, 415–416.

Buijs, J.T., van der Horst, G., van den Hoogen, C., Cheung, H., de Rooij, B., Kroon, J., Petersen, M., van Overveld, P.G.M., Pelger, R.C.M., van der Pluijm, G., 2012. The BMP2/7 heterodimer inhibits the human breast cancer stem cell subpopulation and bone metastases formation. Oncogene 31, 2164–2174.

Chang, C., Holtzman, D.A., Chau, S., Chickering, T., Woolf, E.A., Holmgren, L.M., Bodorova, J., Gearing, D.P., Holmes, W.E., Brivanlou, A.H., 2001. Twisted gastrulation can function as a BMP antagonist. Nature 410, 483–487.

Cho, K.W., Kim, J.Y., Song, S.J., Farrell, E., Eblaghie, M.C., Kim, H.J., Tickle, C., Jung, H.S., 2006. Molecular interactions between Tbx3 and Bmp4 and a model for dorsoventral positioning of mammary gland development. Proc. Natl. Acad. Sci. U. S. A. 103, 16788–16793.

Danielson, K.G., Oborn, C.J., Durban, E.M., Butel, J.S., Medina, D., 1984. Epithelial mouse mammary cell line exhibiting normal morphogenesis in vivo and functional differentiation in vitro. Proc. Natl. Acad. Sci. U. S. A. 81, 3756–3760.

DeOme, K.B., Faulkin, L.J., Bern, H.A., Blair, P.B., 1959. Development of mammary tumors from hyperplastic alveolar nodules transplanted into gland-free mammary fat pads of female C3H mice. Cancer Res. 19, 515.

Dulbecco, R., Henahan, M., Armstrong, B., 1982. Cell types and morphogenesis in the mammary gland. Proc. Natl. Acad. Sci. 79, 7346–7350.

Finak, G., Bertos, N., Pepin, F., Sadekova, S., Souleimanova, M., Zhao, H., Chen, H., Omeroglu, G., Meterissian, S., Omeroglu, A., Hallett, M., Park, M., 2008. Stromal gene expression predicts clinical outcome in breast cancer. Nat. Med. 14, 518–527.

Fleming, J.M., Ginsburg, E., Goldhar, A.S., Plant, J., Vonderhaar, B.K. 2012. Progesterone receptor activates Msx2 expression by downregulating TNAP/Akp2 and activating the Bmp pathway in EpH4 mouse mammary epithelial cells. PLoS ONE 7, e34058.

Gavrieli, Y., Sherman, Y., Ben-Sasson, S.A., 1992. Identification of programmed cell death in situ via specific labeling of nuclear DNA fragmentation. J. Cell Biol. 119, 493–501.

Gazzerro, E., Deregowski, V., Stadmeyer, L., Gale, N.W., Economides, A.N., Canalis, E., 2006. Twisted gastrulation, a bone morphogenetic protein agonist/antagonist, is not required for post-natal skeletal function. Bone 39, 1252–1260.

Graham, A., Koentges, G., Lumsden, A., 1996. Neural crest apoptosis and the establishment of craniofacial pattern: an honorable death. Mol. Cell. Neurosci. 8, 76–83.

Hens, J.R., Dann, P., Zhang, J.P., Harris, S., Robinson, G.W., Wysolmerski, J., 2007. BMP4 and PTHrP interact to stimulate ductal outgrowth during embryonic mammary development and to inhibit hair follicle induction. Development 134, 1221–1230.

Hens, J.R., Wysolmerski, J.J., 2005. Key stages of mammary gland development: molecular mechanisms involved in the formation of the embryonic mammary gland. Breast Cancer Res. 7, 220–224.

Hovey, R.C., Trott, J.F., 2004. Morphogenesis of mammary gland development. Adv. Exp. Med. Biol. 554, 219–228.

Humphreys, R.C., Krajewska, M., Krnacik, S., Jaeger, R., Weiher, H., Krajewski, S., Reed, J.C., Rosen, J.M., 1996. Apoptosis in the terminal endbud of the murine mammary gland: a mechanism of ductal morphogenesis. Development 122, 4013–4022.

Jardé, T., Dale, T., 2012. Wnt signalling in murine postnatal mammary gland development. Acta Physiol 204, 118–27.

Khialeeva, E., Lane, T.F., Carpenter, E.M., 2011. Disruption of reelin signaling alters mammary gland morphogenesis. Development 138, 767–776.

Kobielak, K., Pasolli, H.A., Alonso, L., Polak, L., Fuchs, E., 2003. Defining BMP functions in the hair follicle by conditional ablation of BMP receptor IA. J. Cell Biol. 163, 609–623.

Kouros-Mehr, H., Bechis, S.K., Slorach, E.M., Littlepage, L.E., Egeblad, M., Ewald, A.J., Pai, S.-Y., Ho, I.C., Werb, Z., 2008. GATA-3 links tumor differentiation and dissemination in a luminal breast cancer model. Cancer Cell 13, 141–152.

Kouros-Mehr, H., Slorach, E.M., Sternlicht, M.D., Werb, Z., 2006. GATA-3 maintains the differentiation of the luminal cell fate in the mammary gland. Cell 127, 1041–1055.

Kwon, H.-J., Bhat, N., Sweet, E.M., Cornell, R.A., Riley, B.B., 2010. Identification of early requirements for preplacodal ectoderm and sensory organ development. PLoS Genet. 6, e1001133.

Larman, B.W., Karolak, M.J., Adams, D.C., Oxburgh, L., 2009. Chordin-like 1 and twisted gastrulation 1 regulate BMP signaling following kidney injury. J. Am. Soc. Nephrol. 20, 1020–1031.

Larrain, J., Oelgeschlager, M., Ketpura, N.I., Reversade, B., Zakin, L., De Robertis, E.M., 2001. Proteolytic cleavage of Chordin as a switch for the dual activities of Twisted gastrulation in BMP signaling. Development 128, 4439–4447.

Lawson, K.A., Dunn, N.R., Roelen, B.A.J., Zeinstra, L.M., Davis, A.M., Wright, C.V.E., Korving, J.P.W.F.M., Hogan, B.L.M., 1999. Bmp4 is required for the generation of primordial germ cells in the mouse embryo. Genes Dev. 13, 424–436.

Li, G., Robinson, G.W., Lesche, R., Martinez-Diaz, H., Jiang, Z., Rozengurt, N., Wagner, K.U., Wu, D.C., Lane, T.F., Liu, X., Hennighausen, L., Wu, H., 2002. Conditional loss of PTEN leads to precocious development and neoplasia in the mammary gland. Development 129, 4159–4170.

Little, S.C., Mullins, M.C., 2004. Twisted gastrulation promotes BMP signaling in zebrafish dorsal–ventral axial patterning. Development 131, 5825–5835.

Liu, F., Bloch, N., Bhushan, K.R., De Grand, A.M., Tanaka, E., Solazzo, S., Mertyna, P.M., Goldberg, N., Frangioni, J.V., Lenkinski, R.E., 2008. Humoral bone morphogenetic protein 2 is sufficient for inducing breast cancer microcalcification. Mol. Imaging 7, 175–186.

Loh, K., Chia, J.A., Greco, S., Cozzi, S.-J., Buttenshaw, R.L., Bond, C.E., Simms, L.A., Pike, T., Young, J.P., Jass, J.R., Spring, K.J., Leggett, B.A., Whitehall, V.L.J., 2008. Bone morphogenetic protein 3 inactivation is an early and frequent event in colorectal cancer development. Genes Chromosomes Cancer 47, 449 460.

MacKenzie, B., Wolff, R., Lowe, N., Billington Jr., C.J., Peterson, A., Schmidt, B., Graf, D., Mina, M., Gopalakrishnan, R., Petryk, A., 2009. Twisted gastrulation limits apoptosis in the distal region of the mandibular arch in mice. Dev. Biol. 328, 13–23.

Mailleux, A.A., Overholtzer, M., Schmelzle, T., Bouillet, P., Strasser, A., Brugge, J.S., 2007. BIM regulates apoptosis during mammary ductal morphogenesis, and its absence reveals alternative cell death mechanisms. Dev. Cell 12, 221–234.

Malewski, T., Milewicz, T., Krzysiek, J., Gregoraszczuk, E.L., Augustowska, K., 2005. Regulation of Msx2 gene expression by steroid hormones in human non-malignant and malignant breast cancer explants cultured in vitro. Cancer Invest. 23, 222–228.

Massague, J., Seoane, J., Wotton, D., 2005. Smad transcription factors. Genes Dev. 19, 2783–2810.

McCaffrey, L.M., Macara, I.G., 2009. The Par3/aPKC interaction is essential for end bud remodeling and progenitor differentiation during mammary gland morphogenesis. Genes Dev. 23, 1450–1460.

McEvoy, J., Flores-Otero, J., Zhang, J., Nemeth, K., Brennan, R., Bradley, C., Krafcik, F., Rodriguez-Galindo, C., Wilson, M., Xiong, S., Lozano, G., Sage, J., Fu, L., Louhibi, L., Trimarchi, J., Pani, A., Smeyne, R., Johnson, D., Dyer, Michael, A., 2011. Coexpression of normally incompatible developmental pathways in retino-blastoma genesis. Cancer Cell 20, 260–275.

McNally, S., Martin, F., 2011. Molecular regulators of pubertal mammary gland development. Ann. Med. 43, 212–234.

Melnick, M., Petryk, A., Abichaker, G., Witcher, D., Person, A.D., Jaskoll, T., 2006. Embryonic salivary gland dysmorphogenesis in Twisted gastrulation deficient mice. Arch. Oral. Biol. 51, 433–438.

Metallo, C.M., Ji, L., de Pablo, J.J., Palecek, S.P., 2008. Retinoic acid and bone morphogenetic protein signaling synergize to efficiently direct epithelial differentiation of human embryonic stem cells. Stem Cells 26, 372–380.

Miyazono, K., Maeda, S., Imamura, T., 2005. BMP receptor signaling: transcriptional targets, regulation of signals, and signaling cross-talk. Cytokine Growth Factor Rev. 16, 251–263.

Montesano, R., 2007. Bone morphogenetic protein-4 abrogates lumen formation by mammary epithelial cells and promotes invasive growth. Biochem. Biophys. Res. Commun. 353, 817–822.

Nelson, J.F., Karelus, K., Felicio, L.S., Johnson, T.E., 1990. Genetic influences on the timing of puberty in mice. Biol. Reprod. 42, 649–655.

Nosaka, T., Morita, S., Kitamura, H., Nakajima, H., Shibata, F., Morikawa, Y., Kataoka, Y., Ebihara, Y., Kawashima, T., Itoh, T., Ozaki, K., Senba, E., Tsuji, K., Makishima, F., Yoshida, N., Kitamura, T., 2003. Mammalian twisted gastrulation is essential for skeleto-lymphogenesis. Mol. Cell. Biol. 23, 2969–2980.

Oelgeschlager, M., Larrain, J., Geissert, D., De Robertis, E.M., 2000. The evolutionarily conserved BMP-binding protein Twisted gastrulation promotes BMP signalling. Nature 405, 757–763.

Owens, P., Pickup, M.W., Novitskiy, S.V., Chytil, A., Gorska, A.E., Aakre, M.E., West, J., Moses, H.L., 2012. Disruption of bone morphogenetic protein receptor 2 (BMPR2) in mammary tumors promotes metastases through cell autonomous and paracrine mediators. Proc. Natl. Acad. Sci. 109, 2814–2819.

Petryk, A., Anderson, R.M., Jarcho, M.P., Leaf, I., Carlson, C.S., Klingensmith, J., Shawlot, W., O'Connor, M.B., 2004. The mammalian twisted gastrulation gene functions in foregut and craniofacial development. Dev. Biol. 267, 374–386.

Phippard, D.J., Weber-Hall, S.J., Sharpe, P.T., Naylor, M.S., Jayatalake, H., Maas, R., Woo, I., Roberts-Clark, D., Francis-West, P.H., Liu, Y.H., Maxson, R., Hill, R.E., Dale, T.C., 1996. Regulation of Msx-1, Msx-2, Bmp-2 and Bmp-4 during foetal and postnatal mammary gland development. Development 122, 2729–2737.

Pierce, D.F., Johnson, M.D., Matsui, Y., Robinson, S.D., Gold, L.I., Purchio, A.F., Daniel, C.W., Hogan, B.L., Moses, H.L., 1993. Inhibition of mammary duct development but not alveolar outgrowth during pregnancy in transgenic mice expressing active TGF-beta 1. Genes Dev. 7, 2308–2317.

Rasband, W.S., 1997–2011. ImageJ. U.S. National Institutes of Health, Bethesda, Maryland, USA. (Vol).

Richards, R.G., Klotz, D.M., Walker, M.P., DiAugustine, R.P., 2004. Mammary gland branching morphogenesis is diminished in mice with a deficiency of insulin-like growth factor-I (IGF-I), but not in mice with a liver-specific deletion of IGF-I. Endocrinology 145, 3106–3110.

Ross, J.J., Shimmi, O., Vilmos, P., Petryk, A., Kim, H., Gaudenz, K., Hermanson, S., Ekker, S.C., O'Connor, M.B., Marsh, J.L., 2001. Twisted gastrulation is a conserved extracellular BMP antagonist. Nature 410, 479–483.

Satoh, K., Ginsburg, E., Vonderhaar, B.K., 2004. Msx-1 and Msx-2 in mammary gland development. J. Mammary Gland Biol. Neoplasia 9, 195–205.

Satokata, I., Ma, L., Ohshima, H., Bei, M., Woo, I., Nishizawa, K., Maeda, T., Takano, Y., Uchiyama, M., Heaney, S., Peters, H., Tang, Z., Maxson, R., Maas, R., 2000. Msx2 deficiency in mice causes pleiotropic defects in bone growth and ectodermal organ formation. Nat. Genet. 24, 391–395.

Schwertfeger, K.L., 2009. Fibroblast growth factors in development and cancer: insights from the mammary and prostate glands. Curr. Drug Targets 10, 632–644.

Scott, I.C., Blitz, I.L., Pappano, W.N., Maas, S.A., Cho, K.W., Greenspan, D.S., 2001. Homologues of Twisted gastrulation are extracellular cofactors in antagonism of BMP signalling. Nature 410, 475–478.

Shimmi, O., Umulis, D., Othmer, H., O'Connor, M.B., 2005. Facilitated transport of a Dpp/Scw heterodimer by Sog/Tsg leads to robust patterning of the drosophila blastoderm embryo. Cell 120, 873–886.

Singh, A., Morris, R.J., 2010. The Yin and Yang of bone morphogenetic proteins in cancer. Cytokine Growth Factor Rev. 21, 299–313.

Sotillo Rodriguez, J.E., Mansky, K.C., Jensen, E.D., Carlson, A.E., Schwarz, T., Pham, L., MacKenzie, B., Prasad, H., Rohrer, M.D., Petryk, A., Gopalakrishnan, R., 2009. Enhanced osteoclastogenesis causes osteopenia in twisted gastrulation-deficient mice through increased BMP signaling. J. Bone Miner. Res. 24, 1917–1926.

Stingl, J., Emerman, J.T., Eaves, C.J., Kuusk, U., 1998. Phenotypic and functional characterization in vitro of a multipotent epithelial cell present in the normal adult human breast. Differentiation 63, 201–213.

Sun, M., Forsman, C., Sergi, C., Gopalakrishnan, R., O'Connor, M.B., Petryk, A., 2010. The expression of twisted gastrulation in postnatal mouse brain and functional implications. Neuroscience 169, 920–931.

Tsalavos, S., Segklia, K., Passa, O., Petryk, A., O'Connor, M.B., Graf, D., 2011. Involvement of twisted gastrulation in T cell-independent plasma cell production. J. Immunol. 186, 6860–6870.

van Genderen, C., Okamura, R.M., Fariñas, I., Quo, R.G., Parslow, T.G., Bruhn, L., Grosschedl, R., 1994. Development of several organs that require inductive epithelial–mesenchymal interactions is impaired in LEF-1-deficient mice. Genes Dev. 8, 2691–2703.

Virtanen, S., Alarmo, E.-L., Sandström, S., Ampuja, M., Kallioniemi, A., 2011. Bone morphogenetic protein -4 and -5 in pancreatic cancer–novel bidirectional players. Exp. Cell Res. 317, 2136–2146.

Wagner, D.O., Sieber, C., Bhushan, R., Borgermann, J.H., Graf, D., Knaus, P., 2010. BMPs: from bone to body morphogenetic proteins. Sci. Signal 3, p. mr1.

Wang, K., Feng, H., Ren, W., Sun, X., Luo, J., Tang, M., Zhou, L., Weng, Y., He, T.-C., Zhang, Y., 2011a. BMP9 inhibits the proliferation and invasiveness of breast cancer cells MDA-MB-231. J. Cancer Res. Clin. Oncol. 137, 1687–1696.

Wang, N.J., Sanborn, Z., Arnett, K.L., Bayston, L.J., Liao, W., Proby, C.M., Leigh, I.M., Collisson, E.A., Gordon, P.B., Jakkula, L., Pennypacker, S., Zou, Y., Sharma, M., North, J.P., Vemula, S.S., Mauro, T.M., Neuhaus, I.M., LeBoit, P.E., Hur, J.S., Park, K., Huh, N., Kwok, P.-Y., Arron, S.T., Massion, P.P., Bale, A.E., Haussler, D., Cleaver, J.E., Gray, J.W., Spellman, P.T., South, A.P., Aster, J.C., Blacklow, S.C., Cho, R.J., 2011b. Loss-of-function mutations in Notch receptors in cutaneous and lung squamous cell carcinoma. Proc. Natl. Acad. Sci. 108, 17761–17766.

Watson, C.J., Oliver, C.H., Khaled, W.T., 2011. Cytokine signalling in mammary gland development. J. Reprod. Immunol. 88, 124–129.

Wilson, P.A., Hemmati-Brivanlou, A., 1995. Induction of epidermis and inhibition of neural fate by Bmp-4. Nature 376, 331–333.

Xie, J., Fisher, S., 2005. Twisted gastrulation enhances BMP signaling through chordin dependent and independent mechanisms. Development 132, 383–391.

Ye, L., Kynaston, H., Jiang, W.G., 2009. Bone morphogenetic protein-10 suppresses the growth and aggressiveness of prostate cancer cells through a Smad independent pathway. J. Urol. 181, 2749–2759.

Zakin, L., De Robertis, E.M., 2004. Inactivation of mouse Twisted gastrulation reveals its role in promoting Bmp4 activity during forebrain development. Development 131, 413–424.

Zhang, H., Bradley, A., 1996. Mice deficient for BMP2 are nonviable and have defects in amnion/chorion and cardiac development. Development 122, 2977–2986.

Zhang, J.-L., Patterson, L.J., Qiu, L.-Y., Graziussi, D., Sebald, W., Hammerschmidt, M., 2010. Binding between crossveinless-2 and Chordin Von Willebrand factor type C domains promotes BMP signaling by blocking chordin activity. PLoS ONE 5, e12846.

Zhang, Z., Song, Y., Zhao, X., Zhang, X., Fermin, C., Chen, Y., 2002. Rescue of cleft palate in Msx1-deficient mice by transgenic Bmp4 reveals a network of BMP and Shh signaling in the regulation of mammalian palatogenesis. Development 129, 4135–4146.

Zusman, S.B., Wieschaus, E.F., 1985. Requirements for zygotic gene activity during gastrulation in Drosophila melanogaster. Dev. Biol. 111, 359–371.